Journal of Dynamic Systems, Measurement and Control. Received December 08, 2015;
Accepted manuscript posted September 22, 2016. doi:10.1115/1.4034779

Dynamics and control of a differential drive robot with wheel slip: application to coordination of multiple robots

Shyamprasad Konduri
Graduate Research Assistant,
Student Member of ASME
Department of Mechanical Engineering
Texas A and M University
College Station, Texas 77843
Email: konduri@tamu.edu

Edison Orlando Cobos Torres
Graduate Research Assistant,
Student Member of ASME
Department of Mechanical Engineering
Texas A and M University
College Station, Texas 77843
Email: orlando.cobos@tamu.edu

Prabhakar R. Pagilla*
Professor, Fellow of ASME
Department of Mechanical Engineering
Texas A and M University
College Station, Texas 77843
Email: ppagilla@tamu.edu

ABSTRACT

In differential drive robots wheel slip severely affects the ability to track a desired motion trajectory, and the problem is exacerbated when differential drive robots are used in applications involving coordination of multiple robots. This problem is investigated and based on the wheel-ground traction forces a simple slip avoidance control strategy is discussed. Differential drive robots with two driven wheels and one or more ball-type caster wheels are considered. The traction forces between the wheels and the ground surface are determined by assuming rigid wheel, rigid ground interaction. These traction forces are used to determine the maximum value of the input wheel torque that can be applied on the wheel before it slips. To avoid wheel slip, this limiting torque value is used to set a saturation limit for the input torque computed by a trajectory tracking controller. Stability of the closed loop system

*Address all correspondence related to ASME style format and figures to this author.

with the slip avoidance strategy is shown. Experiments are conducted with this strategy using a single robot as well as multiple robots in a platoon. A representative sample of the experimental results are presented and discussed.

1 Introduction

Research related to wheeled mobile robots (WMR) in a variety of areas, such as modeling, control design, coordination, has been active for over two decades. Because of their simplicity in construction and dynamics, differential drive mobile robots have been commonly used. A typical differential drive robot consists of two driven wheels and one or more caster wheels. Most of the research in differential drive robots has assumed pure rolling of wheels, that is, all the torque provided to the wheels is used to impart motion [1]. In practice, the pure rolling assumption does not always hold, especially in cases where large wheel accelerations are used. When a wheel slips only a portion of the applied torque to the wheels is utilized toward the linear motion of the wheel. Wheel slip can cause considerable deviation from the actual position of a WMR from its desired position. In particular, this deviation is exacerbated when measurements from encoders are used to control the wheel angular position which in turn is used to control the Cartesian position and orientation of the WMR. Wheel slip is unavoidable in differential drive robot because a differential velocity between the two driven wheels is commanded to achieve WMR orientation in the plane.

There have been several studies related to wheel slip in differential drive robots [2–9], wherein the kinematics and dynamics of the WMR under slip are derived. Wheel slip can occur in the longitudinal and/or lateral direction of the wheel motion depending on the wheel acceleration and the traction forces between the wheel and the ground. Traction force expressions are derived for a particular type of wheel-ground interaction and they could be complex depending on the wheel and ground properties. Various combinations of wheel ground interactions have been studied in the literature. For instance a flexible wheel, rigid ground or rigid wheel, flexible ground interaction was used in [2, 3] while other work such as [4, 5], considered rigid wheel, rigid ground interaction. Some studies employ empirical wheel-ground interaction force relations that are found based on extensive experimentation for various conditions.

Several studies in literature have proposed control laws for differential drive robots with wheel slip. In [4] a two stage controller is employed for trajectory tracking. Traction forces are determined by using the static friction coefficient between the wheel and the ground for both slip and non-slip conditions in [5]. An optimal model predictive controller was used to control the differential drive robot when subjected to wheel slippage in [7]. Regulation and turning controllers were developed in [6] using a dynamic model that includes lateral and longitudinal wheel slip. In [8] the lateral slip is added as a nonlinear perturbation to the system and in [9] slip is considered as an uncertainty and estimated. A majority of the controllers proposed in the literature lack experimental validation. Some models involve the use of empirical force models which may require considerable testing for individual wheel and surface conditions which may not be relevant once the surface conditions change. Therefore, a simpler and effective method to eliminate the effect of wheel slip that depends on easily measurable parameters would be useful.

In robot coordination applications where formations are achieved and maintained, the effect of wheel slip is magnified. In vehicle platoons, a spacing error may propagate along the platoon. To correct these spacing errors, each robot may have

to rapidly accelerate and decelerate leading to wheel slip which in turn may exacerbate the spacing errors. Recent work that considered wheel slip in formation control problems may be found in [10, 11]. In [10] an artificial potential function was used to create an adaptive formation control law for systems with lateral slip and parameter uncertainties. Effect of wheel slip in a leader follower type formation controller was explored in [11] to show that slip may cause instabilities in otherwise stable formations.

In this work we study the differential drive robot under wheel slip along with the forces acting at the wheel ground interaction. The maximum force that can be applied on the wheel before it slips is determined and used as a saturation limit on the input wheel torque computed by the controller. Analysis is carried out to determine the effect of this saturation limit on the closed loop stability of the system using an extension of the classical path following controller from [1]. Experiments are conducted to establish that the proposed method is useful in eliminating wheel slip, thereby improving motion coordination performance. The rest of the paper is organized as follows. Mobile robot setup and some preliminary work is discussed in Section 2. A trajectory tracking controller for the differential drive robot along with saturation effect on avoidance of wheel slip is discussed in Section 3. Uncertainty in the coefficient of friction and two methods used to overcome it are discussed in Section 4. Experiments and related discussion using a single robot and a platoon with three mobile robots are presented in Section 5. Section 6 summarizes the work and draws some conclusions.

2 Wheel Slip in Mobile Robots

Consider the sketch of a differential drive robot shown in Fig. 1. Let the position and orientation of the robot center of mass (c) be given by the vector $[x_c, y_c, \phi]^T$. The center of rotation of the two drive wheels are joined together with a rigid link perpendicular to the wheel's plane of rotation. The length of this link is called the wheel base of the robot ($2b$) and its midpoint is the center of rotation of robot (o). The distance from centers of rotation and caster wheel to the center of mass are d and e respectively. The mass and radius of the wheel are m and r, respectively, and the total mass of the robot is m_t. The generalized position vector of the robot is $q = [x_c, y_c, \phi, \theta_R, \theta_L]^T$ where θ is the angle subtended by the wheel w.r.t its vertical axis. The control inputs are the wheel torques (τ_R, τ_L). Let $s_\phi = \sin\phi$ and $c_\phi = \cos\phi$.

The dynamics of the robot in pure rolling (without slip) are given by

$$\dot{v}_x = \frac{1}{m} F_{vx}, \quad \dot{\omega} = \frac{1}{I_t} \tau_\omega. \tag{1}$$

where v_x and ω are longitudinal and angular velocities of the robot, respectively, F_{vx} and τ_ω are the longitudinal force and the angular torque on the robot respectively. The dynamics of the robot when the pure rolling conditions are relaxed and wheels slip in both longitudinal and lateral direction are derived in [12]. For a wheel that is moving in the longitudinal direction under pure rolling, assuming that each wheel of the robot bears half the total weight of the robot, the traction force on the

wheel (F_{wheel}) for applied shaft torque τ are related by the following equation,

$$F_{wheel} = \frac{\tau m_t r}{2I_{wy} + m_t r^2}. \tag{2}$$

The maximum force that has to be applied on the free wheel before it starts to slip is

$$F_{max} = \mu_s N \tag{3}$$

where μ_s is the static friction coefficient and N is the normal reaction. Once the wheel starts to slip the amount of force that is utilized towards the linear motion of the wheel is given by $F_{lin} = \mu_k N$, where μ_k is the kinetic friction coefficient. The difference between the applied force (Equation (2)) and the force F_{lin} causes the wheel to continue slipping. Using these traction forces if we limit the applied torques on the wheels such that the reaction force is less than the maximum allowable force F_{max}, slip can be avoided. Thus, the maximum torque that can be applied to the wheel to avoid slip, is obtained by equating Equation (2) to the value $\mu_s N$, which results in

$$\tau_{max} = \frac{\mu_s N(2I_{wy} + m_t r^2)}{m_t r}. \tag{4}$$

3 Trajectory tracking controller

The control strategy for the robot consists of two loops one nested inside the other. The outer loop controller is used to correct the position errors and the inner loop controls the individual wheel velocities. Let the reference trajectory for the robot center of rotation be (x_r, y_r, ϕ_r) and the corresponding velocities that achieve this trajectory be denoted by (v_{xr}, ω_r). If the actual position of the robot center of rotation is (x, y, ϕ), then the absolute position error is defined as

$$e = [x_r - x,\ y_r - y,\ \phi_r - \phi]^T.$$

Journal of Dynamic Systems, Measurement and Control. Received December 08, 2015;
Accepted manuscript posted September 22, 2016. doi:10.1115/1.4034779

Let $E = [x_e, y_e, \phi_e]^T$ be the position error obtained by transforming e into the robot's reference frame using the coordinate transformation:

$$E = \begin{bmatrix} x_e \\ y_e \\ \phi_e \end{bmatrix} = \begin{bmatrix} \cos\phi & \sin\phi & 0 \\ -\sin\phi & \cos\phi & 0 \\ 0 & 0 & 1 \end{bmatrix} \begin{bmatrix} x_r - x \\ y_r - y \\ \phi_r - \phi \end{bmatrix}. \tag{5}$$

Differentiating (5) gives the error dynamics,

$$\dot{E} = \begin{bmatrix} \dot{x}_e \\ \dot{y}_e \\ \dot{\phi}_e \end{bmatrix} = \begin{bmatrix} \omega_d y_e - v_d + v_{xr}\cos\phi_e \\ -\omega_d + v_{xr}\sin\phi_e \\ \omega_r - \omega_d \end{bmatrix}. \tag{6}$$

We will prove the stability of the outer loop and inner loop separately starting with the proof of the outer loop. Consider the following well known trajectory tracking control law for the outer loop [1]:

$$v_d = v_{xr}\cos\phi_e + k_x x_e \tag{7a}$$

$$\omega_d = \omega_r + v_{xr}(k_y y_e + k_\phi \sin\phi_e) \tag{7b}$$

where d represents the desired velocity, k_x, k_y, k_ϕ are positive controller gains. We wish to show that $(x_e, y_e, \phi_e) = (0,0,0)$ is a stable equilibrium of the system (6) when using the control law (7) for all $v_{xr} > 0$. Let

$$V = \frac{1}{2}(x_e^2 + y_e^2) + (1 - \cos\phi_e)/k_y$$

be a candidate Lyapunov function. V is positive for all non-zero errors (i.e., $V > 0$ for all $E \neq 0$) and zero only when error is zero ($V = 0 \iff E = 0$). The derivative of V is

$$\dot{V} = -k_x x_e^2 - v_r k_\phi \sin^2\phi_e / k_y.$$

$\dot{V}$ is negative definite around the equilibrium point, i.e., $\dot{V} < 0$ for all $((|x_e|, \phi_e) \neq (0, n\pi), n = 0, \pm 1, \pm 2, ...)$. Convergence of y_e to zero is also guaranteed by LaSalle's invariance principle. Hence, $E = 0$ is a uniformly asymptotically stable equilibrium point of $\dot{E} = 0$.

Let the inner loop controller be as follows:

$$\left.\begin{aligned} F_{vx} &= m\dot{v}_d + k_p v_e + k_i \int v_e dt \\ \tau_\omega &= I\dot{\omega}_d + k_p \omega_e + k_i \int \omega_e dt \end{aligned}\right\} \tag{8}$$

where k_p and k_i are positive gains. To show the stability of the inner loop consider the error in the linear and angular velocities: $v_e = v_d - v_x,\ \omega_e = \omega_d - \omega$. Differentiating the linear velocity error and substituting v from (1) and F_{vx} from (8) we obtain

$$\dot{v}_e = -\frac{1}{m}\left(k_p v_e + k_i \int v_e dt\right). \tag{9}$$

Differentiating again we obtain

$$m\ddot{v}_e + k_p \dot{v}_e + k_i v_e = 0. \tag{10}$$

Therefore, the gains k_p and k_i may be selected to obtain the desired velocity error response. Similarly, we can show that

$$I\ddot{\omega}_e + k_p \dot{\omega}_e + k_i \omega_e = 0.$$

Notice that in the inner loop controller the terms $m\dot{v}_d$ and $I\dot{\omega}_d$ are the feed-forward terms added to the output of a simple PI controller. The control inputs from equations (7) and (8) are all implementable as they depend only on the measured and reference variables.

The individual motor torques are calculated from F_{vx} and τ_ω as

$$\tau_R = \frac{r}{2}\left(F_{vx} + \frac{\tau_\omega}{b}\right),\ \tau_L = \frac{r}{2}\left(F_{vx} - \frac{\tau_\omega}{b}\right) \tag{11}$$

A saturation limit using equation (4) is applied on the input torques in the above equation. The block diagram of the entire

closed loop system is shown in Fig. 2. In the preceding we have shown that the closed loop system is stable using the control laws from equations (7) and (8) without input saturation. It is yet to be shown that the system is stable with the addition of the saturation. The following lemma from [13] is useful in proving local exponential stability for the system (1) with saturation.

Lemma 1. *Consider the system*

$$\dot{x} = Ax + B\sigma(u) + d \tag{12}$$

where x is the state vector, A and B are system and input matrices, respectively, d is an external disturbance, and σ is a saturation function. Suppose (A,B) is stabilizable and A has no eigenvalues with strictly positive real parts, then there exists a smooth function $\alpha(x)$ and a positive real number l such that $|\alpha(x)| \leq l|x|$, and the system given by (12) *with $u = \alpha(x)$ is zero-input locally exponentially stable (LES), and its state satisfies an asymptotic bound from $\mathbb{R}^n$ with linear gain and nonzero restriction.*

Consider the dynamics in equation (1), for strictly longitudinal motion, written in terms of the wheel torques we have

$$\left.\begin{aligned} \dot{v}_x &= \frac{1}{mr}(\tau_L + \tau_R) \\ \dot{\omega} &= \frac{b}{rI}(\tau_L - \tau_R) \end{aligned}\right\}. \tag{13}$$

We will show that for longitudinal motion ($\omega = 0$) the system is stable with saturation on input (τ_R and τ_L). With this dynamics, the corresponding matrices used in (12) are

$$A = \begin{bmatrix} 0 & 0 \\ 0 & 0 \end{bmatrix}, B = \begin{bmatrix} 1/mr & 1/mr \\ b/rI & -b/rI \end{bmatrix}, d = \begin{bmatrix} 0 \\ 0 \end{bmatrix}.$$

In order to prove the stability of the system with saturated input one has to show that the pair (A,B) is stabilizable, A has no positive eigenvalues, and the control inputs (11) are bounded. Let

$$K = \begin{bmatrix} k_{11} & k_{12} \\ k_{21} & k_{22} \end{bmatrix}.$$

Journal of Dynamic Systems, Measurement and Control. Received December 08, 2015;
Accepted manuscript posted September 22, 2016. doi:10.1115/1.4034779

Then,

$$A+BK=\begin{bmatrix} \frac{(k_{11}+k_{21})}{mr} & \frac{(k_{12}+k_{22})}{mr} \\ \frac{b(k_{11}+k_{21})}{rI} & -\frac{b(k_{12}+k_{22})}{rI} \end{bmatrix}.$$

The characteristic equation of $(A+BK)$ is

$$\lambda^2+\lambda\left(\frac{b}{rI}(k_{12}+k_{22})-\frac{1}{mr}(k_{11}+k_{21})\right) - \frac{2b}{mr^2I}(k_{12}+k_{22})(k_{11}+k_{21})=0. \tag{14}$$

The roots of the above equation have non positive real parts if k_{11} and k_{21} are chosen such that

$$(k_{11}+k_{21})\leq 0. \tag{15}$$

Therefore, the pair (A,B) is stabilizable. Hence, the conditions for Lemma 1 are satisfied, so there exists a bounded smooth function $\alpha(x)$ which makes system (1) LES and its states v and ω satisfy an asymptotic bound from $\mathbb{R}^n$ with linear gain and nonzero restriction. We still need to show that for a smooth and bounded reference trajectory the linear and angular control torques F_{vx} and τ_w are smooth and bounded.

Since the velocity errors v_e and ω_e are bounded and exponentially decreasing functions, the integrals of those errors are also bounded. Differentiating $\dot{v}_d$ from equation (7), we obtain

$$\dot{v}_d=\dot{v}_{xr}\cos\phi_e-v_{xr}\sin\dot{\phi}_e+k_x\dot{x}_e.$$

Since all the components of $\dot{v}_d$ are bounded, $\dot{v}_d$ is also bounded. Hence, F_{vx} is bounded and the gains k_x, k_p and k_i can be chosen such that the bound is within the saturation value. Along similar lines we can also show that τ_ω is bounded. Notice that we have used the linearized no-slip dynamics in proving the stability with saturation. This is applicable because the dynamics do not include slip as long as the input wheel torques stay below the maximum allowable torque (τ_{max}) obtained in (4).

4 Coefficient of friction μ

The maximum allowable torque calculated in (4) depends on the coefficient of static friction. In the current work, coefficients of friction between the wheel and ground pair for the analysis are obtained experimentally. The robot is pulled on the desired surface and the forces required to start moving the wheels and to keep the wheels moving are measured. These measured forces and calculated normal reaction force (N) on the wheels is used to compute the coefficients. Multiple trails are conducted in different areas of the surface. The resulting values of static and kinetic coefficient of friction obtained are shown in Fig. 3. The mean value of static and kinetic friction coefficients thus obtained are $\mu_s = 0.241$ and $\mu_k = 0.239$. Since the two values are very close to each other and the measurement process is prone to uncertainties for all practical purposes both values are taken to be equal to 0.24.

The value of μ varies considerably for a wheel and surface pair depending on the operating conditions. Environmental factors like dust, spills, etc., can cause these variations. If these uncertainties are not accounted for in the experiments they may produce discrepancies in the results. The following are two methods considered to account for these uncertainties while performing the experiments. (1) One can choose a value for μ that is smaller than the measured or expected value of μ to account for the uncertainty. For instance, if the measurements of μ has a 20% uncertainty, then using a conservative value of $0.8\mu_o$ (μ_o being the base value) for experiments will guarantee that irrespective of what μ is within the uncertain region the wheels do not slip. However, such an estimate further limit the range of torques that can be used. (2) Another strategy is to obtain an online estimate of μ using velocity and position measurements. Generally, to accurately estimate the friction coefficient position sensors are required in addition to the wheel encoders. This is not always possible and in such situations encoder measurements can be used to get rough estimates, as long as the applied input torque is well below the maximum allowable torque (since τ close to τ_{max} may cause the wheels to slip). The relation between input torque τ, wheel rotational acceleration α and friction coefficient μ_s is given by

$$\tau = I_{wy}\alpha + r\mu_s N. \tag{16}$$

The maximum allowable torque (τ_{max}) corresponds to a maximum allowable acceleration (α_{max}) which can be computed using the above relation. Similarly one-half of the τ_{max} also corresponds to an acceleration which can be computed from measurements using the wheel encoders. Hence, the relation (16) can be used to verify if the estimated value of μ used is acceptable and can be adjusted in the event it is not. In this paper we have used the first approach of utilizing a value for μ that is smaller than the measured value to obtain torque saturation limit.

5 Experiments using Single Robot and Platoons

Each wheeled mobile robot has two independent wheels and a free-ball caster wheel, Fig. 4. Each independent wheel is fixed to the shaft of the motor rated at 12 V, with a no-load speed of 350 rotations per minute and a stall torque of 0.78 m-N. A pair of quadrature encoders with 1856 counts per revolution mounted on the shaft of the motor are used to measure the

speed of the wheels and calculate the position of the robot. The robot control algorithms are implemented using an Arduino micro-controller along with motor drivers and 'Xbee Series 1' communication module and a desktop computer containing a 'Xbee Series 1' as receiver.

The robot parameter values are $2b$ = 0.21 m, e = 0.095 m, d = 0.055 m, g = 9.81 m/s, h = 0.0216 m, m_r = 1.5 kg, I_r = 0.009753 kg m^2, I_{wz} = 0.000584 kg m^2, I_{wy} = 0.001168 kg m^2, r = 0.0365 m, m_w = 0.064 kg. Using these numerical values, the maximum allowable torque on each wheel is found to be 0.095 m-N which is equivalent to an acceleration of approximately 45 rad/s^2; this is applied as a saturation between the computed input torque and the drive motors, see Fig. 2. Model simulations and experiments are conducted to verify the dynamics and the traction force relations and are shown in [12].

To test the effect of saturation, the wheels are accelerated for about 0.5 seconds using a constant input torque after which the torque is set to zero (i.e., constant velocity). The position of the robot is calculated using the encoder readings and the actual position of the robot is obtained using the overhead video camera. The maximum available motor torque of 0.13 m-N is used to accelerate the robot. The positions of the robot from both encoders and video with and without saturation on the torque input are shown in Fig. 5(a). When input torque is not saturated the encoders over estimate the robot position; this is because the eoncders measure the angular displacement and do not account for wheel slip. When the input torque is restricted to less than 0.095 m-N the position obtained from both encoder and video match each other. Such a torque limiting strategy will be applied in the coordination experiments next.

Coordination experiments are conducted with three robots in a platoon with and without the slip avoidance strategy for each robot. The reference position of the robot q_{ref} is obtained by the combination of the neighbor vehicles' position q_{i-1} and the desired inter-vehicular spacing δ_i as $q_{ref} = q_{i-1} - \delta_i$. The communication between the robots follows a ring structure. The robot positions through out the experiments are obtained from the encoders and the final positions are measured manually.

The experiment started with zero inter-vehicular spacing error and the coordination controller is started after 3 seconds into the experiment. The starting position for robots are (0.6096, 0), (0,0) and (-0.6096, 0) meters with zero degree orientation. The desired inter-vehicular spacing is set to 0.6096 m. The velocity profile used for the experiments is shown in Fig. 6. The evolution of the x-position of the robots without and with limiting the torque are shown in Fig. 5(b). Notice that the rate of change of position follows the desired velocity profile. Notice that when input torques are limited, the positions change more smoothly than without such torque limits, in particular during accelerations and decelerations. Also observe that when limiting input wheel torque, the inter-vehicular spacings are maintained better. The evolution of y-positions for both cases is shown in Fig. 5(c). Observe that the error in the y-position is much smaller when the torque limiting strategy is employed. The final positions of the three robots from encoder and manual measurement without limiting torque are (4.78, 0.02), (4.17, 0.04), (3.55, 0.03) and (4.87, 0.24), (4.26, 0.18), (3.65, 0.42). The x-positions are within 0.1 meters whereas the y-position has larger error. The final positions with slip avoidance are (4.97, 0.003), (4.36, 0.005), (3.75, 0.002) and (5.02, 0.07), (4.38, 0.06), (3.77, 0.06); clearly the errors in both x and y are much smaller. When input torques are saturated using τ_{max}, wheel slip is avoided thereby improving the accuracy of position measurement and reducing the spacing errors.

6 Conclusion

In this work we have investigated wheel slip and its effect on coordination of multiple mobile robots. The traction forces between the wheel and ground are used to create a saturation limit on the input wheel torques to avoid slip. Simulation and experimental results involving single and multiple robots in coordination are used to show the effect of such a saturation. The analysis in Section 3 shows that input saturation does not effect the stability of the closed loop system with an appropriate choice of the controller gains. From the experimental results it can be observed that a simple saturation on the input wheel torques is effective in increasing the reliability of measurements from the encoders. Future work will include online estimation of friction coefficients using an additional position sensor. The current work mostly involved straight line trajectories, future work will involve using curvilinear paths which give rise to lateral wheel slip.

References

[1] Kanayama, Y., Kimura, Y., Miyazaki, F., and Noguchi, T., 1990. "A stable tracking control method for an autonomous mobile robot". In Proceedings of IEEE International Conference on Robotics and Automation, pp. 384–389 vol.1.

[2] Balakrishna, R., and Ghosal, A., 1995. "Modeling of slip for wheeled mobile robots". *IEEE Transactions on Robotics and Automation,* **11**(1), pp. 126–132.

[3] Tian, Y., Sidek, N., and Sarkar, N., 2009. "Modeling and control of a nonholonomic wheeled mobile robot with wheel slip dynamics". In IEEE Symposium on Computational Intelligence in Control and Automation, pp. 7–14.

[4] Albagul, A., Wahyudi, and Wahyudi, 2004. "Dynamic modeling and adaptive traction control for mobile robots". In Proceedings of 30th Annual Conference of IEEE Industrial Electronics Society, Vol. 1, pp. 614–620 Vol. 1.

[5] Nandy, S., Shome, S., Somani, R., Tanmay, T., Chakraborty, G., and Kumar, C., 2011. "Detailed slip dynamics for nonholonomic mobile robotic system". In International Conference on Mechatronics and Automation, pp. 519–524.

[6] Tian, Y., and Sarkar, N., 2014. "Control of a mobile robot subject to wheel slip". *Journal of Intelligent and Robotic Systems,* **74**(3-4), pp. 915–929.

[7] Wei, S., Uthaichana, K., Zefran, M., and Decarlo, R., 2013. "Hybrid model predictive control for the stabilization of wheeled mobile robots subject to wheel slippage". *IEEE Transactions on Control Systems Technology,* **21**(6), Nov, pp. 2181–2193.

[8] Burghi, T. B., Iossaqui, J. G., and Camino, J. F., 2015. "Stability analysis of perturbed nonlinear systems applied to the tracking control of a wheeled mobile robot under lateral slip". In Proc. of the XVII International Symposium on Dynamic Problems of Mechanics.

[9] Hoang, N.-B., and Kang, H.-J., 2014. "An adaptive tracking controller for differential wheeled mobile robots with unknown wheel slips". In *Intelligent Computing Theory*, D.-S. Huang, V. Bevilacqua, and P. Premaratne, eds., Vol. 8588 of *Lecture Notes in Computer Science*. Springer International Publishing, pp. 277–284.

[10] Ze-su, C., Jie, Z., and Jian, C., 2012. "Formation control and obstacle avoidance for multiple robots subject to wheel-slip". *Int J Adv Robot Syst,* **9**.

[11] Tian, Y., and Sarkar, N., 2012. "Formation control of mobile robots subject to wheel slip". In IEEE International

Conference on Robotics and Automation (ICRA), pp. 4553–4558.

[12] Torres, E. C., Konduri, S., and Pagilla, P., 2014. "Study of wheel slip and traction forces in differential drive robots and slip avoidance control strategy". In American Control Conference (ACC).

[13] Teel, A. R., 1996. "A nonlinear small gain theorem for the analysis of control systems with saturation". *IEEE Trans. on Automat. Contr.,* **41**(9), pp. 1256–1270.

List of Figures

Journal of Dynamic Systems, Measurement and Control. Received December 08, 2015;
Accepted manuscript posted September 22, 2016. doi:10.1115/1.4034779

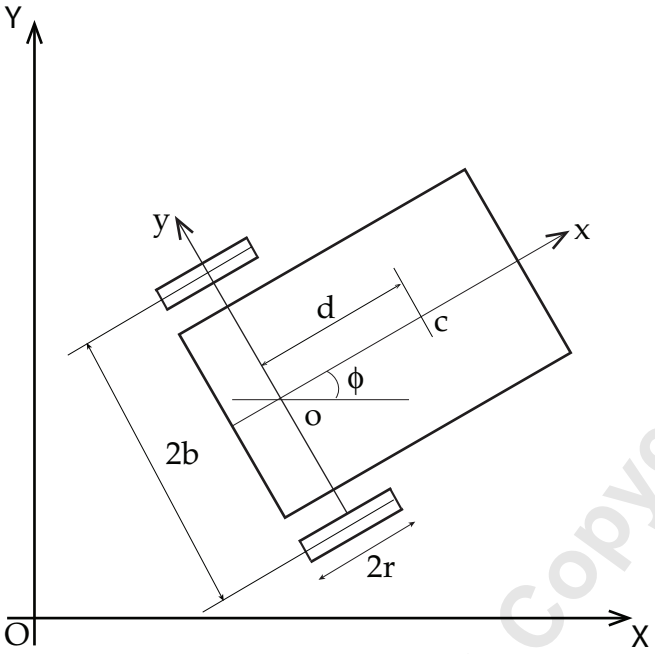

Fig. 1: Two Wheeled Differential Drive Robot

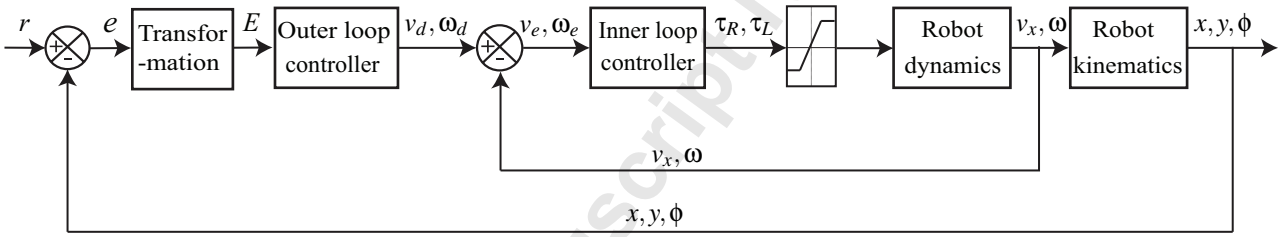

Fig. 2: Two loop trajectory tracking controller.

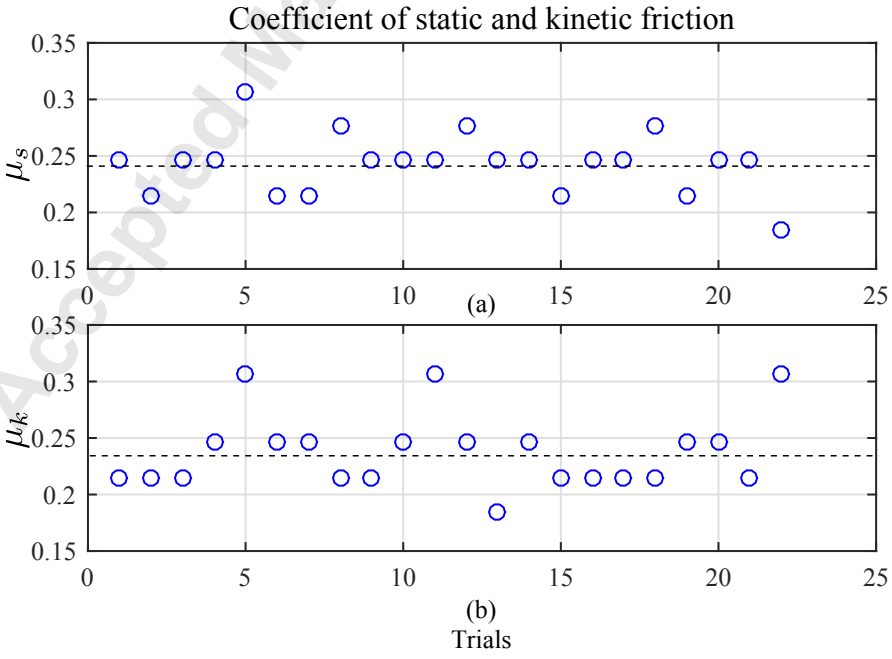

Fig. 3: Experimental values of coefficient of friction (a) μ_s and (b) μ_k.

Journal of Dynamic Systems, Measurement and Control. Received December 08, 2015;
Accepted manuscript posted September 22, 2016. doi:10.1115/1.4034779

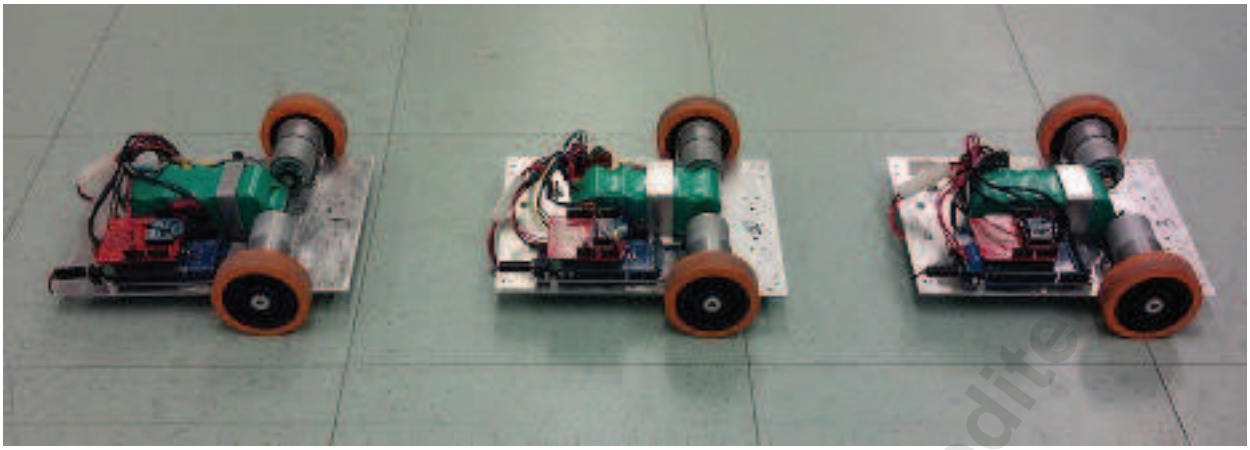

Fig. 4: Picture of mobile robots in platoon.

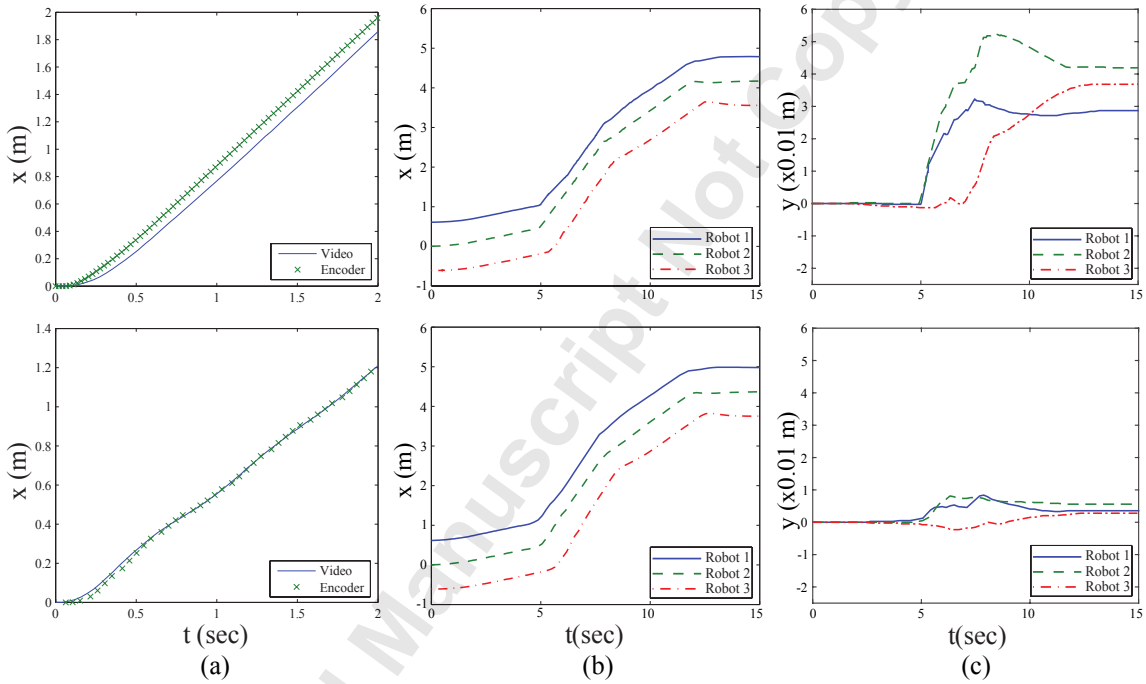

Fig. 5: Evolution of the position of the robot (a) single robot from encoder and video without and with limits on torque input, platoon of robots without and with limit on torque input (b) x-position, (c) y-position.

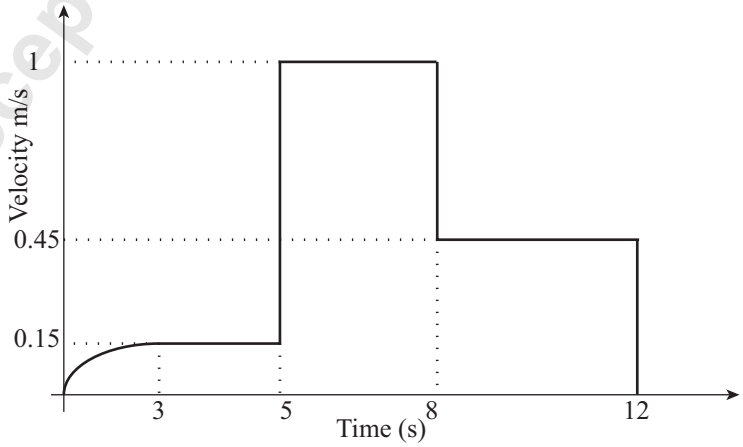

Fig. 6: Velocity profile used in experiments.